Comparison of DSMC and Euler Equations Solutions for Inhomogeneous Sources on Comets.

Susanne Finklenburg[a], Nicolas Thomas[a], Jörg Knollenberg[b], Ekkehard Kührt[b]

[a]*Universiät Bern, Physikalisches Institut, Siedlerstrasse 5, 3012 Bern, Switzerland*
[b]*DLR, Rutherfordstrasse 2, 12489 Berlin, Germany*

Abstract. Cometary activity arises from the sublimation of surface ices into the gas phase. Dust is entrained in the gas and is accelerated by gas drag as the gas escapes into interplanetary space. Previous observations [1, 2] of cometary nuclei have shown remarkable, diverse structures in the near-nucleus dust distribution. The gas from the comet expands into vacuum and the flow therefore passes through a wide range of densities and pressures and hence though different flow regimes. While a direct simulation Monte Carlo (DSMC) simulation [3] should give, in all cases, accurate results if applied correctly, the calculation becomes slow in denser regions. Solving the Euler equations (EE) is in these cases faster, but they are only an approximation for dilute gas. A direct comparison between DSMC and EE was made by Lukianov et al. [4] for water vapor subliming from an ice sphere into vacuum. He found that the Euler equation with correct boundary conditions gives a good approximation to the velocity and density field in the supersonic region even at global Kn > 10^{-3}.We have performed further comparisons of the DSMC and EE methods for a case with an 'active cap': A region with a half opening angle of 10° has twice the production rate compared with the rest of the sphere. We found that far away from the active cap, the flow is like one from a sphere and our results are in a very good agreement with Lukianov et al.'s [4]. However the Euler equations start to fail close to and at the sides of the jet produced by the active area at lower Knudsen numbers.

Keywords: Comets, near nucleus atmosphere, DSMC, Euler equation
PACS: 96.25.Fx

INTRODUCTION

In 2014 the European Space Agency spacecraft Rosetta will arrive at comet 67P/Churyumov-Gerasimenko. Onboard is a camera system OSIRIS, which will observe the nucleus and the surrounding dust coma at spatial scales down to 2 cm/px [5]. The near nucleus gas distribution will be observed by a combination of experiments including MIRO, a microwave spectrometer [6] and the mass spectrometer ROSINA [7].

Cometary nuclei are small having a typical diameter of a few kilometers and irregular shapes. From Hubble observations [8], diameters of 3-5 km are estimated for 67P/Churyumov-Gerasimenko. For ground-based observations, the nucleus is difficult to observe directly because of dust emission. This leads to the need for spacecraft observations in situ such as those that will be provided by Rosetta. Our aim is to interpret the appearance of structures in the dust and gas coma and to prepare for the data analysis phase of Rosetta starting in 2014. We particularly wish to understand the relationship between surface activity and the gas and dust distribution in the inner coma.

The activity of a comet is produced by the sublimation of water ice and therefore depends strongly on the distance to the sun which provides the energy source to drive the sublimation. Dust is entrained in the gas and is accelerated by gas drag as the gas escapes into interplanetary space. The dust acts to (partially) obscure the surface from view. The Rosetta spacecraft will go into orbit around the comet and accompany it from 4 astronomical units through to perihelion. To plan the observations it is necessary to understand and interpret observations quickly so that the results can be used to plan follow-up sequences. It is also a special situation because the boundary conditions are not well known: E.g. there are contradicting interpretations regarding the thermal conductivity of the surface [9, 10] and it is unclear where exactly the sublimating ice is. There may be regions which are enriched in water or CO ice or the observed structures in the gas flow may be an effect of the surface topography [11, 12]. From observations of other comets it is also known that nuclei have irregular shapes and that their surfaces have a very low albedo (about 4%). Hence, precise determination of outgassing characteristics prior to arrival at the comet is hardly possible. In order to give an order of magnitude estimation for the sublimation rate of comet 67P/Churyumov-Gerasimenko, we use here the model cases defined by Tenishev et al. [13]. All instruments on

Rosetta should be switched on once the comet reaches 3.25 AU. A dayside water outward flux of approx. 10^{17} m^{-2} s^{-1} is assumed at this time and on the nightside $5x10^{15}$ $m^{-2}s^{-1}$ with surface temperatures of 182 K and 139 K, respectively. Perihelion is at 1.29 AU. At this time the water flux is assumed to be $3x10^{20}$ $m^{-2}s^{-1}$ and 10^{19} $m^{-2}s^{-1}$ on the dayside and nightside respectively with temperatures of 196 K and 172 K.

MODEL DEVELOPMENT

The goal of this work is to find a way to simulate the dusty gas flow in the near nucleus region. Because of the ill-defined conditions at the surface, there is no need for accurate specification of input parameters. However, the gas and dust flow structures which one might predict could, even at this stage, provide constraints for the mission. We are interested in the region from the surface, out to about one nucleus radius above the surface.

As a first step we calculated the axially symmetric flow from spheres with regions with different activity using the DSMC program DS2V written by G.A. Bird [3] (Version 4.5.05). We have compared this to an Euler equation solver [14].

Typically the sublimation flow from a sphere is characterized in terms of the (global) Knudsen number Kn.

$$Kn = \frac{\lambda}{L} = \frac{1}{\sqrt{2}\pi d_{ref}^2 n_w}\left(\frac{T_w}{T_{ref}}\right)^{\omega-0.5}\frac{1}{L} \tag{1}$$

Here λ is the mean free path calculated from the number density n_w and the temperature T_w given as boundary conditions and L the radius of the sphere. The formula for the mean free path given here is for VHS (variable hard sphere) molecules [15]. The reference diameter (d_{ref}=6.15x10^{-10} m) at the reference temperature (T_{ref}=*300 K)* and the exponent of the temperature in the viscosity law (ω=*1.1)* are the model parameters. The given values are for water vapor [16].

Directly over the surface the gas is assumed to have a half space Maxwell-Boltzmann distribution with temperature T_w and number density n_w. The outflow from the surface is then according to the Hertz-Knudsen equation

$$Q = \sqrt{\frac{kT_w}{2\pi m}}n_w \tag{2}$$

(Q: particle flow [$m^{-2}s^{-1}$], m=18 u≈3x10^{-26} kg, molecular mass for water, k=1.38x10^{-23} J/K Boltzmann constant) This results in number densities between n_w=5x10^{13} m^{-3}, Kn=4 (at 3.25 AU, night side) and n_w=3x10^{18} m^{-3}, Kn=9x10^{-5} (at 1.29 AU, day side). Note that this formula gives only the outflow part. If the flow is not free molecular, there is backscattering and the net outflow as well as the velocity is reduced. This point will be discussed in more detail in the next section. Although the global Knudsen number is, in the present case, not a good criterion for the choice of the simulation/calculation method the number gives an idea about the density regime close to the surface. A traditional way to estimate the region in a comet coma where the gas can be described by fluid dynamics models is the "collision zone": This is the region around the nucleus where the local mean free path of the gas is smaller than the distance to the centre of the nucleus. Assuming that the density is inversely proportional to the radius squared the radius of the collision zone (expressed in units of nucleus radii) is inversely proportional to the global Knudsen number.

ANALYTICAL RESULTS FOR THE FLOW FROM A SPHERE IN THE FREE MOLECULAR AND THE FLUID CASE

The formulae given in this paragraph are taken from Sone [17].

In case of the free molecular flow ($Kn = \infty$), the distribution function of the gas is known:

$$f(r,v,\theta) = \begin{cases} n_w\left(\frac{m}{2\pi kT_w}\right)^{3/2}\exp\left(-\frac{mv(\theta)^2}{2kT_w}\right) & for\ 0 \le \theta < \arcsin(L/r) \\ 0 & otherwise \end{cases} \tag{3}$$

The *v(θ)* are the velocities which are on a circular cone with an opening angle of θ. L is the radius of the source sphere. The macroscopic variables can then be calculated in the usual way by solving the moment integrals:

$$\frac{n}{n_w} = \frac{1}{2}\left[1 - \sqrt{1 - \left(\frac{L}{r}\right)^2}\right] \tag{4}$$

$$\frac{T}{T_w} = 1 - \frac{2}{3\pi}\left[1 + \sqrt{1 - \left(\frac{L}{r}\right)^2}\right]^2 \tag{5}$$

$$\frac{v}{\sqrt{2k/mT_w}} = \frac{1}{\sqrt{\pi}}\left[1 + \sqrt{1 - \left(\frac{L}{r}\right)^2}\right] \tag{6}$$

In the case of a fluid flow ($Kn = 0$), one uses the law for adiabatic expansion, energy and mass conservation over each sphere and the definition of the Mach number, M, to get the following results:

$$\frac{T}{T_*} = \frac{2/(\gamma-1)+1}{2/(\gamma-1)+M^2} \tag{7}$$

$$\frac{n}{n_*} = \left(\frac{2/(\gamma-1)+1}{2/(\gamma-1)+M^2}\right)^{1/(\gamma-1)} \tag{8}$$

$$\frac{u}{\sqrt{2k/mT_*}} = \sqrt{\frac{\gamma}{2}} M \sqrt{\frac{2/(\gamma-1)+1}{2/(\gamma-1)+M^2}} \tag{9}$$

$$\frac{r}{L_*} = \frac{1}{\sqrt{M}}\left(\frac{2/(\gamma-1)+1}{2/(\gamma-1)+M^2}\right)^{-\frac{\gamma+1}{4(\gamma-1)}} \tag{10}$$

γ is the ratio of the specific heats for the given gas. The index * is used for the parameter values at the $M = 1$ surface. Note that there is a subsonic region around the sphere even in the case of a small Knudsen number: $L_* > L$.

The values of T_*, n_* and the fraction of backscattered molecules (b) for polyatomic gases were calculated by Cercignani [18]. For a gas with 3 internal degrees of freedom he finds: $T_*/T_w = 0.814$, $n_*/n_w = 0.299$, $b = 0.219$. The idea behind these values is that the velocity distribution function in the Knudsen layer is a linear combination of the half space Maxwellian close to the surface and an equilibrium distribution at an infinite distance. In the evaporation flow from a sphere, the existence of an equilibrium region depends on the global Knudsen number.

Looking again at the problem to estimate the initial number density n_w from a measured flux at an arbitrary distance, in Eq. (2) the backscattered molecules were neglected. If one corrects for this effect, the number density is about 30% larger than without.

TEST CASES AND METHODS

Two different flow fields, homogeneous sphere and "ActiveCap", were simulated with two different methods: DSMC and the Euler equations solver (EE). Considerable effort was invested to ensure compatible simulation conditions. We took advantage of rotational symmetry in both programs.

In the DSMC simulation, the gas leaves the surface of the sphere with a half space Maxwellian with the parameters n_w and T_w. All molecules hitting the surface are adsorbed. The gas is assumed to have 3 internal degrees of freedom. The energy transfer between internal and translational degrees of freedom is calculated with the Larsen-Borgnakke model [19] and a rotational relaxation collision number of 1 [20]. The total simulation region has a size of 5 km x 10 km and the sphere of 2 km radius is located at the origin. The situation is shown in Fig. 1. The lower boundary is here the rotation axis. The boundary on the left side is a plane of symmetry which reflects all simulation molecules specularly. All molecules are removed from the simulation if they cross one of the other two boundaries (vacuum).

In the EE calculation, the simulation region is larger, going out to 20 km from the center of the sphere. The entering gas is calculated as if it would come through a nozzle having sonic speed at the surface. The boundary conditions are given by a gas production rate and the temperature of the imaginary subsurface reservoir. Cercignani's temperature and density ratios were used to calculate the matching boundary conditions.

In a first step, the flow from a homogeneous sphere was calculated. This was mainly done to understand and match the boundary conditions of the two programs and to check for numerical artifacts along the rotation axis. There were no significant errors found. The results from these tests will not be described in more detail here.

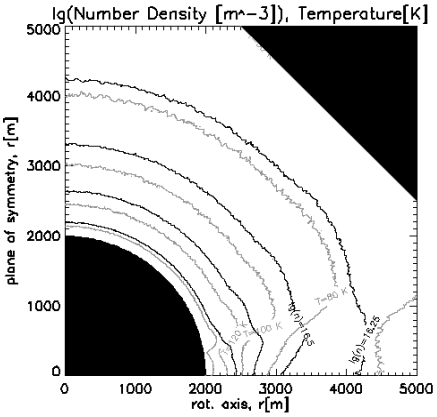

FIGURE 1. The DSMC simulation result for the ActiveCap case. In black: density contours with n = (1, 0.18, 0.32 and 0.56) 10^{17} m^{-3}. In gray: temperature contours with T = (140, 120, 100, 80, 60) K. The circle segment represents the nucleus, the black triangle in the upper right corner is a region which was excluded from the simulation region.

Both codes were used with grid sizes successfully tested in [14] for the EE code and in [3] and [21] for DS2V, respectively.Here, the "ActiveCap" case will be discussed: Around the symmetry axis, there is an active area with a half opening angle of 10°. In this active area the number density n_w is twice as large as on the rest of the sphere. (see Fig. 1 for typical density and temperature contours). In order to cover the possible flow regimes at comets representing different distances from the sun, the flow was calculated with different densities (see Table 1). The number in the test case name indicates by which factor the density is lower compared to the "ActiveCap" case: e.g. the initial gas density in "ActiveCap-2" if ½ of the one in "ActiveCap". Everything else is the same for all cases: The initial gas temperature is T_w=195.5K and the sphere a radius of L=2 km.

RESULTS

The "ActiveCap" case allows us to study the flow from a homogeneous sphere in addition to the effects of the active cap itself: We look at the flow far away from the active region (i.e. close to the plane of symmetry or the y-axis in our simulations). The gas flow in this region allows us to evaluate different boundary matching strategies.

Gas sublimating from a sphere into vacuum, when close to the surface, is never in a local thermal equilibrium (LTE) and always subsonic. On expansion, it becomes supersonic and may relax towards LTE which is lost again further out (depending on Kn). [4][17]

The analytical EE solution as well as the EE solver cannot describe the subsonic region. Therefore the gas parameters at the sonic line have to be used as boundary conditions. There are two possibilities shown and discussed here: On the one hand we use Cercignani's [18] results (used in the EE solver, too), on the other hand the results of our DSMC simulation. Both can be found in Table 1. Cercignani's values are given in the first line. For each of the "ActiveCap" cases, number density, translational temperature and distance to the center of the "nucleus" were read out along the sonic line between 0°-5° to the rotational axis for the cap and 20°-90° to the rotational axis for the flow from a sphere. The averages of these two groups are given in Table 1.

The number density ratio depends only very slightly on the Knudsen number. In the case of the translational

TABLE 1. The different DSMC cases and the calculated parameter ratios. The left value in each column is the one for the active area and the right hand value is that of the rest of the surface. n_w: initial number density (parameter of the initial VDF); Kn: Knudsen number, see Equ. (1); T_w=195.5 K; L=2 km; Index * for values at the sonic surface; L_*/L-1: width of the subsonic region in units of the nucleus radius.

Name	n_w [$10^{18}m^{-3}$]	Kn	n_*/n_w	T_*/T_w (transl.)	L_*/L-1
Fluid ([18])		0	0.299	0.814	
ActiveCap	1/0.5	2.3e-4/4.6e-4	0.31/0.31	0.78/0.78	0.017/0.011
ActiveCap-2	0.5/0.25	4.6e-4/9.2e-4	0.30/0.30	0.78/0.78	0.024/0.016
ActiveCap-5	0.2/0.1	1.2e-3/2.3e-3	0.30/0.30	0.78/0.78	0.037/0.024
ActiveCap-10	0.1/0.05	2.3e-3/4.6e-3	0.30/0.30	0.78/0.77	0.048/0.031
ActiveCap-100	0.01/0.005	2.3e-2/4.6e-2	0.32/0.32	0.72/0.70	0.077/0.049
ActiveCap-1000	0.001/0.005	2.3e-1/4.6e-1	0.34/0.34	0.65/0.64	0.063/0.048
Free molecular		∞	0.351	0.643	0.0474

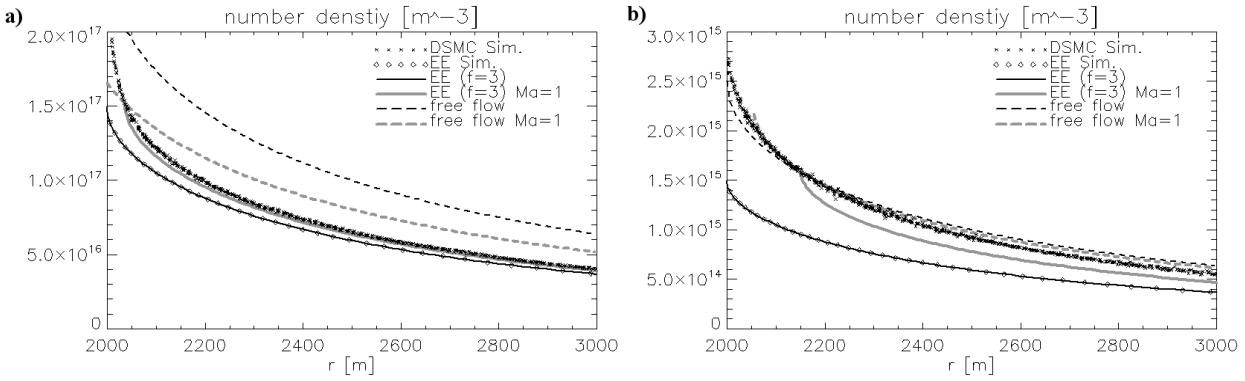

FIGURE 2. The number density in cases a)ActiveCap and b)ActiveCap-100 (small dots) along a line with a 85°angle to the rotation axis.

temperature the differences are larger (see Table 1). This was also found for the gas over the active region and is in a very good agreement with Lukianov et al.'s [4, 22] results. The main difference between the parameters over the active cap and the rest of the surface is in the thickness of the subsonic layer (L_*/L-1 in Table 1). Note that while the density and temperature ratios have values between the two "extreme" cases (fluid and free molecular flow) the subsonic layer is thicker at Kn ≈ 10^{-2} than in the free molecular case ([17] and [4], Fig. 10). This is because the density, velocity and temperature ratios at a fixed point close to the surface are not a monotonic function of the initial number density

Figure 2 shows the number density as a function of the radius in the region where the flow is like the flow from a homogeneous sphere (85° angle to the rotation axis). The simulation results are shown with dots for the DSMC ("DSMC Sim.") and squares for the EE ("EE Sim.") while the analytical results are given as black lines. The dashed lines show the results for the free molecular flow (Eq. (4)) ("free flow"), the solid ones the result of Eq. (8) and (10) with $\gamma=8/6$. This is the analytical Euler solution with 3 internal degrees of freedom ("EE (f=3)"). Grey are the lines where n_w, T_w resp. n_*, T_* and L_* were chosen to produce the DSMC results at the sonic line.

Figure 2a) shows the situation for ActiveCap where the (global) Knudsen number is small enough that one expects some agreement with the fluid solution close to the nucleus. From r ≈ 2500m (r/L=1.25) on outwards the numerical results show this expected agreement. Closer to the nucleus, there is the small subsonic layer in the DSMC result (22 m, see Table 1), for which the EE cannot give a useful result. In the region in-between, the agreement can be improved if results from the DSMC solution are used to calculate the boundary conditions.

In Fig. 2b) the same curves are shown for the ActiveCap-100 case. As expected the DSMC results are close to the free molecular solution. However in the subsonic region the DSMC results are larger than both analytical ("extreme") cases. This is the result of the local maximum in the thickness of the subsonic layer. If one uses again results from the DSMC simulation as boundary conditions for the calculation, the free flow solution shows, as

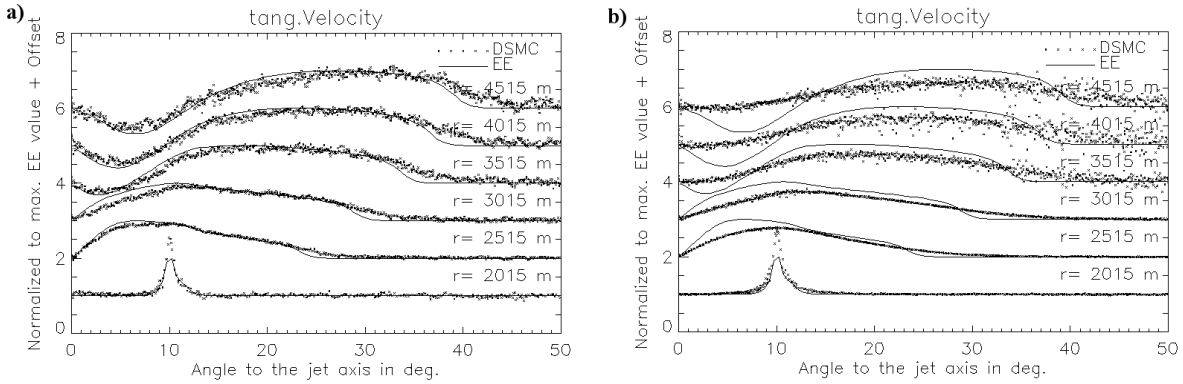

FIGURE 3. The velocity parallel to the surface of the sphere in different distances to the surface (at 2000 m). Figure a) shows the situation for the ActiveCap case, figure b) for ActiveCap-5. Note that the values are normalized to the maximum value in the EE solution at the given radius and for each radius a different offset is added (always +1). A positive velocity points away from the active region, a negative one into it. With the added offset, a negative velocity is here one that it below its offset level (e.g. values lower than 6 in this figure represent negative velocities in a distance of 4515 m from the centre of the nucleus).

expected, a slightly higher density.

The result from the analytical solution of the EE and the EE solver agree in both cases perfectly as expected. Note that the differences in density and velocity between the two analytical solutions is, in the shown region, less than 20% (for the temperature the difference is up to 50%) if they have the same parameters at the sonic surface. This is probably better than the uncertainties in our knowledge of the boundary conditions at present.

Structures in the dust distribution appear mostly where the gas flow has a velocity component parallel to the surface. This velocity component is shown for different distances to the centre of the nucleus, r, in Fig. 3.

The solid lines are the numerical results of the EE and the dots represent the DSMC results. The maximum value in the EE solution with which both results (DSMC and EE) are normalized is 40 m/s at r=2015, 70 m/s at r=2515 m and drops to 17 m/s at 4515 m.

Figure 3a) shows the results of the case ActiveCap, Fig. 3b) the ones of ActiveCap-5. Although the density difference is only a factor 5, the consequences are obvious: While there is a quite good agreement between the two solutions in the first figure this is not the case in the second one: There is no velocity back to the jet axis and also most of the other structures are lost. A quite good agreement between DSMC and EE exists in the case ActiveCap, but when the density drops the mean free path increases, the local Knudsen number increases and one can observe the rarefaction effect.

CONCLUSIONS

The subsonic region close to the nucleus needs to be simulated with DSMC. In the case of a fairly homogeneous flow, one can estimate the gas parameters at the sonic line but differences are largest close to this surface and in our case, this is most probably the region where the dust is influenced the most.

Without larger gradients than simply the ones due to the expansion, the supersonic flow can be calculated to the first approximation by using either a free molecular approach or the Euler equations. This fails as soon as smaller scale structures in a rarefied gas appear. In this case the local Knudsen number increases and the theoretical non-usability of the Euler equations becomes obvious. The Navier-Stokes equations may extend the region where a fluid solution gives acceptable results for us. In the future, we will need to calculate in 3-D because of the detailed shape of the nucleus and will also have to include gases other than H_2O as well as dust.

REFERENCES

1. H.U. Keller et al., *Images of the Nucleus of Comet Halley*, ESA-SP 1127, Vol. 1, pp.1
2. T.L. Farnham, *Icarus* **191**, 146-160 (2007)
3. G.A. Bird, Molecular Gas Dynamics and the Direct Simulation of Gas Flows, Oxford, Clarendon Press, 1994
4. G.A. Lukianov, G.O. Knanlarov, *Thermosphysics and Aeromechanics* **7**, 489-498 (2000)
5. Keller et al., *SSR* **128**, 433 (2007)
6. Gulkis et al., *SSR* **128** (2007)
7. Balsiger et al., *SSR* **128** (2007)
8. P.L. Lamy, et al., *Astronomy and Astrophysics*, **458**, 669-678 (2006)
9. O. Groussin, et al., *Icarus* **191**, 63-72 (2007).
10. B. Davidsson, et al., *Icarus* **201**, 335-357 (2009).
11. J.M. Sunshine, et al., *Science* **311**, 1453-1455 (2006)
12. Crifo, et al., "Nucleus-Coma Structural Relationships" in Comets II, edited by M. Festou et al., Tucson: University of Arizona Press, 2005, pp.491-503
13. V. Tenishev, et al., *Astrophysical Journal* **685**, 659-677 (2008)
14. J. Knollenberg, "Modellrechnungen zur Staubverteilung in der inneren Koma von Kometen", Ph.D. Thesis, Georg-August-Universität Göttingen, 1993.
15. G.A.Bird, *Physics of Fluids* **26**, 3222-3223(1983)
16. J.F.Crifo, *Astron.Astrophys*. **223**, 365-368 (1989) and J.F. Crifo et al., *Icarus* **156**, 249-268 (2002)
17 Y. Sone, H. Sugimoto, *Physics of Fluids A* **5**, 1491-1511 (1993)
18. C. Cercignani, "Strong Evaporation of a Polyatomic Gas" in Rarefied Gas Dynamics, edited by S.Fisher, New York: American Institute of Aeronautics and Astronautics, 1981
19. C. Brorgnakke, P.S. Larsen, *Journal of computational Physics* **18**, 405-420 (1975)
20. M.J. Combi, *Icarus* **123**, 207-226 (1996)
21. G.A. Bird, "Notes from September 30 Short Course at DSMC07", http://sydney.edu.au/engineering/aeromech/dsmc_gab/
22. G.A.Lukyanov et al. "Comparison between Navier-Stokes and DSMC Simulations of the Rarefied Gas Flow from Model Cometary Nuclei" in Rarefied Gas Dynamics, edited by M.Cpitelli, Melville, N.Y.: American Institute of Physics, 2005